Interaction of non-biodegradable particles and granular sludge in Nereda®—— from nanoparticles to microparticles

Peng, Zhaoxu; Piaggio, Antonella L.; Giglio, Guilherme Lelis; Ortega, Sara Toja; van Loosdrecht, Mark C.M.; de Kreuk, Merle K.

DOI
10.1016/j.watres.2025.123698

Publication date
2025

Document Version
Final published version

Published in
Water Research

Citation (APA)
Peng, Z., Piaggio, A. L., Giglio, G. L., Ortega, S. T., van Loosdrecht, M. C. M., & de Kreuk, M. K. (2025). Interaction of non-biodegradable particles and granular sludge in Nereda®—— from nanoparticles to microparticles. *Water Research*, *281*, Article 123698. https://doi.org/10.1016/j.watres.2025.123698

Water Research 281 (2025) 123698

Contents lists available at ScienceDirect

Water Research

journal homepage: www.elsevier.com/locate/watres

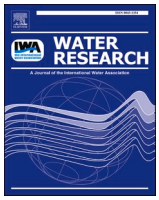

Interaction of non-biodegradable particles and granular sludge in Nereda®—— from nanoparticles to microparticles

Zhaoxu Peng [a,b,*], Antonella L. Piaggio [a], Guilherme Lelis Giglio [a,c], Sara Toja Ortega [a], Mark C.M. van Loosdrecht [d], Merle K. de Kreuk [a]

[a] Faculty of Civil Engineering and Geosciences, Section Sanitary Engineering, Department of Water Management, Delft University of Technology, Stevinweg 1, Delft, South Holland 2628 CN, the Netherlands
[b] School of Water Conservancy and Transportation, Zhengzhou University, Kexue Road 100, Zhengzhou 450001, China
[c] Biological Processes Laboratory (LPB), São Carlos School of Engineering (EESC), University of São Paulo (USP), Brazil
[d] Department of Biotechnology, Delft University of Technology, van der Maasweg 9, Delft 2629 HZ, the Netherlands

ARTICLE INFO

Key words:
Aerobic granular sludge
Microparticles
Filtration
Attachment
Removal efficiency

ABSTRACT

>50 % of the organic matter in sewage consist of particulate chemical oxygen demand (pCOD). This study used 250 μm fluorescent microbeads, 130±58 μm microparticles and 100 nm nanobeads to simulate sewage particles, and investigated the fate of these particles under both plug flow feeding and aeration phases in an aerobic granular sludge (AGS) system. Filtration performance was dominantly influenced by the particle size rather than the upflow velocity (V_{upflow}). The microbeads exhibited 95±3 % filtration efficiency with obvious accumulation around the AGS bed bottom, even as slight fluidization started at the V_{upflow} of 5.0 $m \cdot h^{-1}$. In contrast, the nanobeads filtration efficiency was significantly lower (43±6 %). During the aeration phase, the attachment efficiency increased with the decrease of particle size. The microbeads attachment efficiency variated between 39–49 %, whereas the microparticles and nanobeads achieved better attachment of 89.4–95.2 % and 98.8–99.3 %, respectively. Furthermore, aeration batch tests showed both nanobeads and the irregular microparticles attachment by AGS was strong, and the detach-attach of nanobeads/microparticles between different sized AGS was very limited duration aeration. This work provides insight into the fate of particles in AGS system. The optimal sludge treatment was also evaluated in the scope of this removal of non-biodegradable, and potentially harmful particles.

1. Introduction

Wastewater treatment by conventional activated sludge systems generally require large surface areas due to the poor sludge settleability and low biomass concentration. One of the emerging technologies to overcome the problems is the AGS technology, in which sludge flocs are substituted by compact and fast settling granules (Winkler et al., 2022). In full-scale wastewater treatment plants, the AGS technology under the trade name Nereda® has been applied in >140 plants, which operates in sequencing batch reactors with cycles of simultaneous upflow feeding/discharge, aeration, and settling. One key issue for granulation is to ensure the influent organic matter is maximumly used/stored by the slow-growing bacteria during feeding period (Van Dijk et al., 2022; Elahinik et al., 2022).

However, the organic matters in actual sewage are very complex, which could generally be classified into dissolved chemical oxygen demand (dCOD) and pCOD, and their proportion is mainly determined by the wastewater source (Karahan et al., 2008; Wang et al., 2014). Specifically, the black water contains a higher amount of pCOD than the grey water (Hocaoglu et al., 2013), and the pCOD in municipal wastewater often accounts for >50 % of the total COD. Unlike the dCOD which can diffuse faster and easily be utilized by the heterotrophs (Van den Berg et al., 2022), the pCOD must be attached (colonised as a biofilm) by microorganisms firstly, then be hydrolyzed to dCOD by the extra cellular enzymes, which is often considered the rate limiting step (Toja Ortega et al., 2021). Therefore, the utilization of pCOD in actual wastewater will directly impact the granulation performance in the AGS systems.

The biomass-specific hydrolysis rate of pCOD in the AGS systems was found to be mainly determined by the available granule surface area,

* Corresponding author at: School of Water Conservancy and Transportation, Zhengzhou University, Kexue Road 100, Zhengzhou 450001, China.
E-mail address: pzx@zzu.edu.cn (Z. Peng).

https://doi.org/10.1016/j.watres.2025.123698
Received 24 January 2025; Received in revised form 2 April 2025; Accepted 21 April 2025
Available online 22 April 2025

and the slow-growing bacteria like phosphorus accumulation organisms or glycogen accumulation organisms were abundant around the hydrolytically active sites (Toja Ortega et al., 2022). In a typical Nereda® cycle, part of influent pCOD will be retained by the sludge bed during the anaerobic upflow feeding phase, especially the 1–100 μm microparticles, most of them were accumulated in the first 2.0 cm of the settled sludge bed (Layer et al., 2020). While the nanoparticles could be distributed throughout the sludge bed and immobilized into the granules, even penetrating the outer 300 μm of the granules (Ranzinger et al., 2020). During the aeration phase, most accumulated pCOD will be re-suspended and preferentially attached to the flocs (Layer et al., 2020). Previous research employed the magnetic resonance imaging to explore the distribution of particles within granules, flocs, and void spaces during the upflow feeding process. However, its limited resolution constrained to specifically observe the pCOD, and the analyzable height of sludge bed was also restricted (Van den Berg et al., 2022). In addition, the particle size distribution of pCOD in actual wastewater is very broad (Alvarado et al., 2021), and limit research have systematically investigated the transfer process of all sized pCOD in Nereda® system.

To address the bottleneck above, considering the AGS was academically defined as 200 μm (De Kreuk et al., 2007), and the transfer of biodegradable pCOD will always be influenced by the activity of sludge. In this study, the non-biodegradable fluorescent 250 μm microbeads and 100 nm nanobeads were used to simulate the maximum and minimum pCOD. Their attachment and detachment with AGS and sludge flocs during a typical Nereda® cycle were monitored, using the granules originating from a full-scale Nereda® plant. Firstly, the filtration performance of settled sludge bed during feeding was investigated, as well as the filtration efficiency of differently sized pCOD under different V_{upflow}; Secondly, the interactions (attachment and detachment) of pCOD and biomass during aeration were determined, especially the influence of granule and particle size; Finally, the effect of influent pCOD on the treatment of waste AGS was evaluated.

2. Materials and methods

2.1. AGS source and solution preparation

AGS was collected from Nereda® WWTP Utrecht, in The Netherlands. The designed flow and sludge loading rate were 74,700 $m^3 \cdot d^{-1}$ and 0.05 $kgCOD \cdot kgVSS^{-1} \cdot d^{-1}$, respectively. The AGS mixtures were collected from the bottom of the reactor after a minimum aeration of 30 min to ensure completely mixed condition. The sampled AGS was washed as follows: (i) it was initially diluted with tap water; (ii) followed by 5 min of settling; (iii) and then the supernatant was discharged. The process was repeated multiple times until the supernatant was clear. The distribution of the mixed liquor suspended solids (MLSS) was 11 % (<0.2 mm), 18 % (0.2–1.0 mm), 32 % (1.0–2.0 mm), 23 % (2.0–3.1 mm) and 16 % (> 3.1 mm). The washed AGS mixture was divided into two parts, which were used for the plug flow feeding experiment and batch experiment, respectively.

Three types of particles were used in each experiment: microbeads, microparticles, and nanobeads. Fluorescent green microbeads (Cospheric, WTW D-82,362 Weilheim, Model: SEP 25) with a diameter and density of 250 μm and 1.02 $g \cdot mL^{-1}$, were used to simulate the large non-biodegradable particles of sewage. Three drops (0.05 mL each) of microbeads were diluted in 1.0 L milli-Q water to prepare the microbeads solution for the plug flow feeding experiment (1400±360 $microbeads \cdot L^{-1}$), and ten drops were diluted in 1.0 L miliQ water to prepare solution for the batch experiment, adding up to an average of 5125±450 $microbeads \cdot L^{-1}$. The microparticles solution was prepared by grinding the microbeads into smaller sizes by a mortar and subsequently added into miliQ water. The concentration for the plug flow feeding experiment and batch experiment were 3267±208 $microparticles \cdot L^{-1}$ (130±58 μm) and 7567±907 $microparticles \cdot L^{-1}$ (111±50 μm), respectively. The density of microbeads/microparticles were a little bigger than 1.00 $g \cdot mL^{-1}$, they were not stable and could not be saved for long-term, so the microbeads solution and microparticles solution were prepared two times for the plug flow feeding experiment and batch experiment, respectively. Nanobeads ($Eu(NO_3)_3 \cdot 5H_2O$, CAS No: 100,587–95–9. Jiangsu Zhichuan Technology Co., LTD) with the diameter of 100 nm were diluted with miliQ water to prepare a nanobeads solution with a final concentration of 195±23 $\mu g \cdot L^{-1}$ that was used in both experiments.

2.2. Experimental procedure

2.2.1. Plug flow feeding experiment

The plug flow feeding experiment was carried out in an AGS laboratory-scale reactor with a diameter, height, and working volume of 6.0 cm, 51.3 cm and 1.45 L, respectively. The solution was completely mixed by a magnetic mixer (Labinco BV, Model L 23) and pumped by a peristaltic pump (series 323, Watson Marlow, headquarters) to the bottom of the reactor (Fig. 1). The first part of washed AGS mixture was added with the settled volume around 0.6 L (5 min) and MLSS of 11,140 $mg \cdot L^{-1}$ (calibration to 1.45 L). According to the experience of full-scale Nereda® plant, the typical V_{upflow} was 1.0–1.5 $m \cdot h^{-1}$ in dry weather and 3.0–5.0 $m \cdot h^{-1}$ in wet weather (Pronk et al., 2015), and it usually need 0.5 h to mix the mixture completely after aeration (Toja Ortega et al., 2021). So in this experiment the V_{upflow} increased from 1.0 $m \cdot h^{-1}$ to 5.0 $m \cdot h^{-1}$, and the aeration last for 60 min. The plug flow feeding experiment consisted of feeding phase and aeration phase, the details are described in Table 1. Samples were collected from the effluent and supernatant after feeding, and the mixture around the middle height of reactor at 10 min, 30 min and 60 min of aeration. After taking each sample, an equal volume of milli-Q water was supplied. The reactor was operated for three cycles to treat the solutions of microbeads, microparticles and nanobeads, respectively.

2.2.2. Batch experiment

The batch experiment was carried out in four 1.0 L conical flasks. The washed AGS mixture was sequentially filtered by stainless steel sieves with the pore size of 3.1 mm, 2.5 mm, 2.0 mm, 1.4 mm, 1.0 mm, 0.6 mm and 0.2 mm. To facilitate the comparison between different sized granules, the filtered fractions of <0.2 mm, 0.6–1.0 mm, 1.4–2.0 mm and 2.5–3.1 mm were placed in separate beakers containing miliQ water for later use. Then 50 mL of each settled sludge fraction were sucked by a pipette and put into a conical flask, followed by the addition of 500 mL solution. Therefore, the working volume of each batch test was 0.55 L. The bulk was mixed by aeration with the intensity of 2.0 $L \cdot min^{-1}$ for 60 min. Samples were taken at 10 min, 30 min and 60 min. After taking each sample, an equal volume of milli-Q water was supplied. The batch operation was repeated three times to treat microbeads solution, microparticles solution and nanobeads solution, respectively. The dilution effect have been taken into account in calculation of removal efficiency.

2.3. Analytical procedures

2.3.1. MLSS, porosity and granule morphology

The AGS mixture was sequentially sieved from 3.1 mm to 0.2 mm, and the MLSS was measured for each fraction. The minimum pore of the sieves was the 0.2 mm, since it represented the smallest granules (De Kreuk et al., 2007). MLSS was measured according to standard methods (APHA, 2005). Moreover, the porosity of settled sludge and expansion ratio were measured with the dextran blue method (Beun et al., 2002), and the granule morphology was observed by a digital microscope (VHX-5000). The particle size distribution was determined with a particle size analyzer (Microtrac S3500, Model Bluewave).

2.3.2. Particle concentration

Microbead: The sieves with pore sizes of 3.10 mm, 2.00 mm, 1.00 mm, 0.33 mm and 0.20 mm were stacked from the top to the bottom,

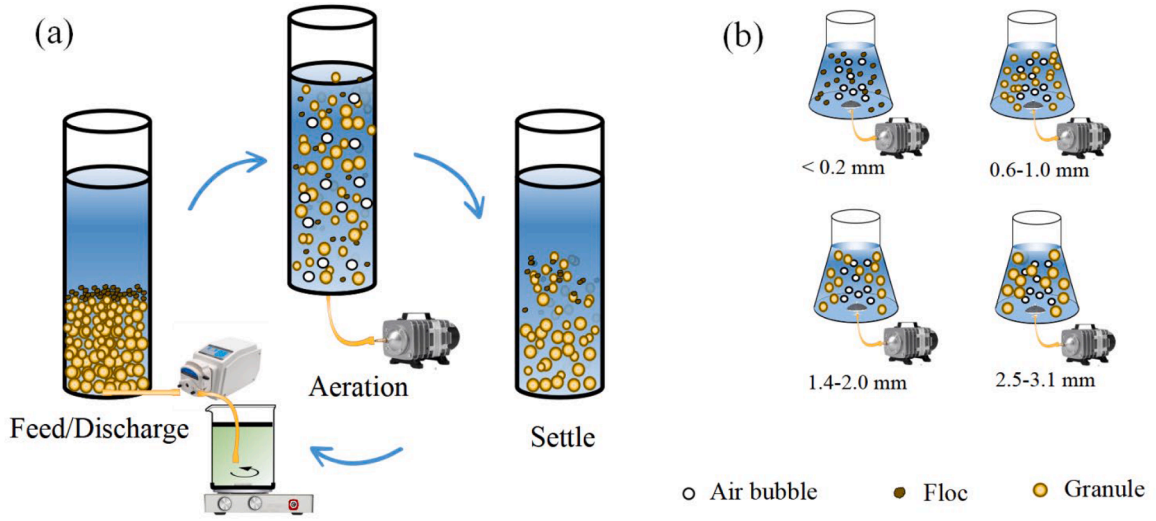

Fig. 1. Experimental set-up. (a) Plug flow feeding experiment; (b) Batch experiment.

Table 1
Conditions implemented in the plug flow feeding experiment.

Feeding Phase								Aeration phase		Settling phase
V_{upflow} ($m \cdot h^{-1}$)	Duration (min)	V_{upflow} ($m \cdot h^{-1}$)	Duration (min)	V_{upflow} ($m \cdot h^{-1}$)	Duration (min)	V_{upflow} ($m \cdot h^{-1}$)	Duration (min)	Aeration flow ($L \cdot min^{-1}$)	Duration (min)	Duration (min)
1.0	30	2.0	15	3.0	10	5.0	6	2.0	60	30

followed by pouring 10.0 mL sample for sequential filtration. The filtered solids were rinsed with tap water while slightly shaking the sieves. The filtered solids on the 0.20 mm sieve were collected and placed onto a glass slide. All visible 250 μm fluorescent microbeads were recorded by digital microscopy, and processed with counting.

Microparticle: The sieves with the same pore sizes described previously were used, except for 0.33 mm. The filtrated solids from each sieve size were picked up and put in four different 10.0 mL centrifuge tubes, followed by the addition of 10.0 mL milli-Q Water, then the samples were treated by ultrasonic at 40 KHz for 5 min to remove microparticles from the biomass. The liquid in each centrifuge tube and the filtered liquid of the 0.20 mm sieve were observed by a digital microscope (VHX-5000). Any observed microparticles were photographed, then all the images were analyzed by a deep learning method to quantify the number, shape and area of the observed microparticles (Jia et al., 2024).

Nanobead: The nanobeads used in this research exhibited fluorescent properties with the excitation wavelength of 360 nm and emission wavelength of 615 nm. A dilution series of nanobeads solution were prepared in miliQ water up to 200 $\mu g \cdot L^{-1}$. The adsorption of light (Excitation Filter 405 nm, Emission filter 590 nm) was measured with a micro plate reader (POLARstar Galaxy bmq) as a calibration line (relative coefficient > 0.99).

2.3.3. Fluorescence staining

The biomass after the nanobeads batch experiment was used to stain as follows: (1) Fix with iced-ethanol at room temperature for 5 min; (2) Take out and equilibrate it in phosphate buffer saline (PBS) for 5 min; (3) Dilute EbbaBiolight 680 (Ebba Biotech) in PBS 1:1000; (4) Take out again and incubate in the diluted EbbaBiolight solution under room temperature for 30 min; (5) Mount the biomass and seal the coverslip onto the slide. The sample was observed by Olympus fluorescence microscope (BX63) with Cy3.5 filter set. The excitation and emission wavelengths were 530 nm and 680 nm, respectively.

2.4. Calculation procedures

During the feeding phase, some particles were filtered by the settled sludge bed, while others stayed in the liquid phase. The filtration performance was calculated as in Eqs. (1) and (2); The retained particles in the pore of settled bed were calculated by Eq. (3); During the aeration phase, the filtrated particles were re-suspended, and some would be attached by granules or flocs. The attachment performance was calculated as in Eqs. (4) and (5):

$$\textbf{Filtered particles} = \left(\Sigma Q_{i-inf} \times T_{i-feed} \times C_{i-inf}\right) - \left(\Sigma Q_{i-effl} \times T_{i-feed} \times C_{i-eff}\right) - V_{i-sup} \times C_{i-sup} \quad (1)$$

$$\textbf{Filtration efficiency}(\%) = 100 \times \text{Filteredparticles} / \left(\Sigma Q_{i-inf} \times T_{i-feed} \times C_{i-inf}\right) \quad (2)$$

$$\textbf{Retained particles in pores of the settled AGS bed} = V_{settled\ sludge} \times P \times (1 + 0.01 \times E) \times C_{i-sup} \quad (3)$$

$$\textbf{Attached particles} = \left(\Sigma Q_{i-inf} \times T_{i-feed} \times C_{i-inf}\right) - \left(\Sigma Q_{i-eff} \times T_{i-feed} \times C_{i-eff}\right) - V_{mixture} \times C_{aeration} \quad (4)$$

$$\text{Attachment efficiency}(\%) = 100 \times \text{Attached particles} / \left(\Sigma Q_{i-inf} \times T_{i-feed} \times C_{i-inf}\right) - \left(\Sigma Q_{i-eff} \times T_{i-feed} \times C_{i-eff}\right) \quad (5)$$

Where:

$Q_{i\text{-}inf}$: the feeding flow under the i^{th} V_{upflow}, $L{\cdot}min^{-1}$;
$T_{i\text{-}feed}$: the feeding duration under the i^{th} V_{upflow}, min;
$C_{i\text{-}inf}$: the concentration of influent particles under the i^{th} V_{upflow}, L^{-1} or $\mu g{\cdot}L^{-1}$;
$Q_{e\text{-}inf}$: the effluent flow under the i^{th} V_{upflow}, $L{\cdot}min^{-1}$;
$C_{i\text{-}eff}$: the concentration of effluent particles under the i^{th} V_{upflow}, L^{-1} or $\mu g{\cdot}L^{-1}$;
$V_{i\text{-}sup}$: the volume of supernatant during feeding under the i^{th} V_{upflow}, L;
$C_{i\text{-}sup}$: the concentration of supernatant particles under the i^{th} V_{upflow}, L^{-1} or $\mu g{\cdot}L^{-1}$;
P: porosity, %; E: expansion ratio, %; $V_{mixture}$: the mixture volume, 1.45 L;
$C_{aeration}$: the concentration of suspended particles during aeration, L^{-1} or $\mu g{\cdot}L^{-1}$;

3. Results

3.1. Effect of V_{upflow} on filtration performance during plug flow feeding

The filtration performance of the settled sludge bed at increasing V_{upflow} from 1.0 $m{\cdot}h^{-1}$ to 5.0 $m{\cdot}h^{-1}$ is shown in Fig. 2. The porosity of the AGS bed after 5 min settling was around 50 %. The pore volume of the 0.61 L AGS settled bed under these up-flow conditions was 0.30 L at V_{upflow} of 1.0 m h^{-1}. At 5.0 $m{\cdot}h^{-1}$ the upper part of the settled AGS bed started to expand slightly, resulting in a bed volume of 0.64 L and a pore volume of 0.32 L. Applying the different up-flow velocities, it was observed that the filtration efficiency decreased with the decrease of particle size, but the percentage of particles retained in the pores of settled AGS bed to the total filtered particles increased with the decrease of particle size. When the V_{upflow} was 1.0 $m{\cdot}h^{-1}$, the filtration efficiencies of microbeads, microparticles and nanobeads were 98 %, 74 % and 53 ±11 %, respectively. For the 250 μm microbeads, most filtered microbeads were accumulated at the bottom of AGS bed, similar to observations by Layer et al. (2020). For the 130±58 μm microparticles, 9.67 % of microparticles which did not flow into the supernatant was retained in the pores of AGS bed. While >34±4 % of nanobeads which did not pass through the AGS bed were retained in the pores. This result is in line with the findings of Ranzinger et al. (2020), also they found that nanobeads would flow throughout the pores of settled sludge bed, and the retained nanobeads were dominantly attached by the settled sludge bed.

The influence of V_{upflow} on the filtration performance of different sized particles was different. For the 250 μm microbeads, the filtration performance decreased with the increase of V_{upflow}. Its filtration efficiencies decreased from 98 % at 1.0 $m{\cdot}h^{-1}$ to 91 % at 5.0 $m{\cdot}h^{-1}$. Actually, obvious microbeads were accumulated around the bottom of AGS bed. The supporting force generated by 5.0 $m{\cdot}h^{-1}$ was so big that the settled AGS bed began to slightly fluidise with the expansion ratio close to 5 %. The increased pore volume provided more space to capture microbeads with retained percentage increased from 1 % to 4 %. For the 130±58 μm microparticles, the filtration performance was not affected by V_{upflow}. The filtration efficiency was 75±4 % under the V_{upflow} of 1.0–5.0 $m{\cdot}h^{-1}$, and the microparticles retained in the pores of AGS bed was 9±2 %. For the small 100 nm nanobeads, none were accumulated around the bottom and the filtration performance was the best when V_{upflow} was 1.0 $m{\cdot}h^{-1}$, then the filtration efficiency dropped from 53±11 % to 43±1 % when V_{upflow} increased to 2.0–5.0 $m{\cdot}h^{-1}$, leading to the retained percentage decreased from 34±4 % to 11±3 %.

3.2. Effect of particle size on particle — AGS interaction during aeration after plug-flow feeding

It can be expected that during the aeration phase, the particles attached by the settled AGS bed partially detach, and the particles accumulated at the bottom or retained in the pores of settled AGS bed will be released into the bulk liquid. Meanwhile, the particles in the bulk liquid could also attach to the AGS through random collision. The attachment of different sized particles to the AGS during aeration is shown in Fig. 3. The attachment efficiency refers to the ratio of the attached particles to the total particles in the mixture, and it increased with the decrease of particle size. The average attachment efficiencies of 250 μm microbeads, 130±58 μm microparticles and 100 nm nanobeads were 45±5 %, 92±3 % and 99±0.3 %, respectively.

The 250 μm microbeads, with their spherical shape and smooth

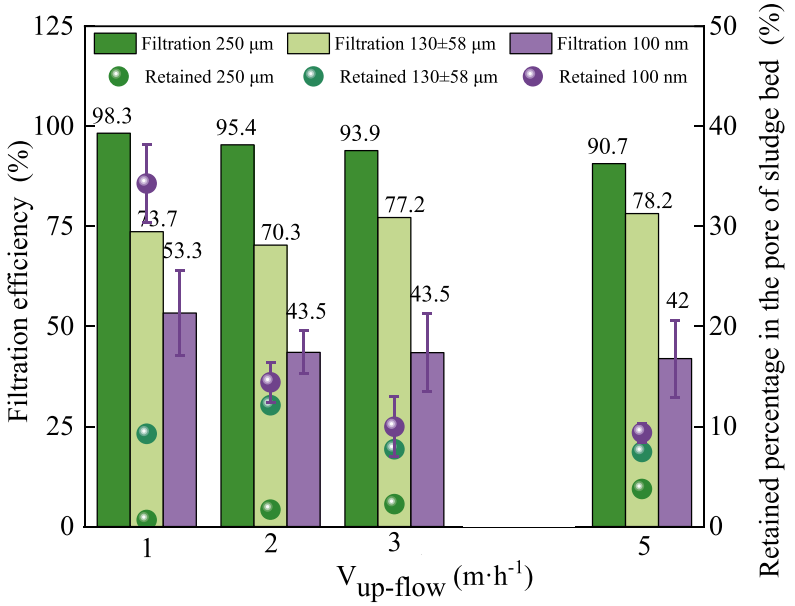

Fig. 2. Filtration performance of settled sludge bed for different sized particles under different V_{upflow}.

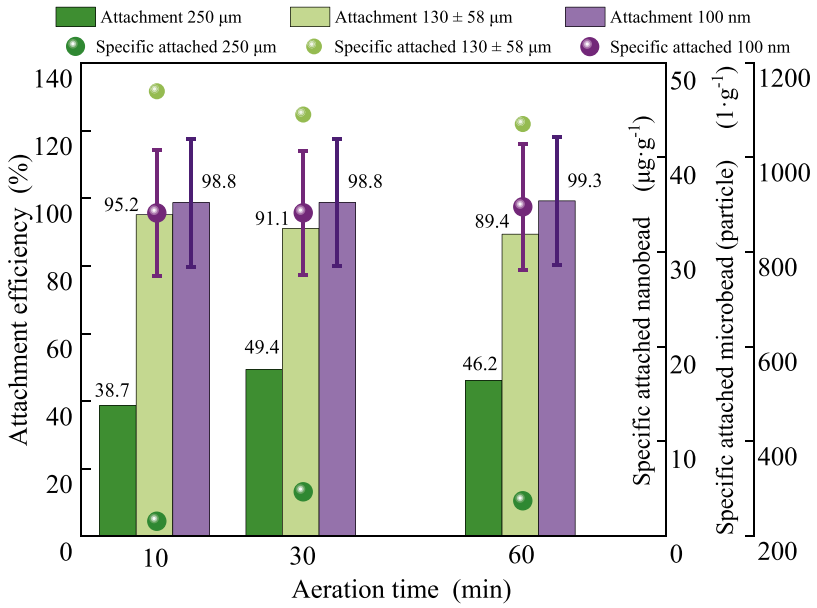

Fig. 3. Attachment performance between AGS mixture and different sized particles during aeration after plug-flow feeding.

surface, exhibited a low attachment efficiency ranging from 39 % to 49 %. While most 130±58 μm microparticles already attached at the beginning of aeration phase, and their attachment efficiency slightly decreased from 95 % after 10 min aeration to 89 % at 60 min aeration. It seemed these rough surface and irregular sharp shaped microparticles strongly connected to the AGS, and they were difficult to be detached upon aeration (Fig. 5(c)). The average specific attached microparticles during aeration was 1100±36 microparticles·g^{-1}, which was almost 4 times bigger than that of 250 μm microbeads (260±32 microbeads·g^{-1}). Similarly, most 100 nm nanobeads were also already attached after 10

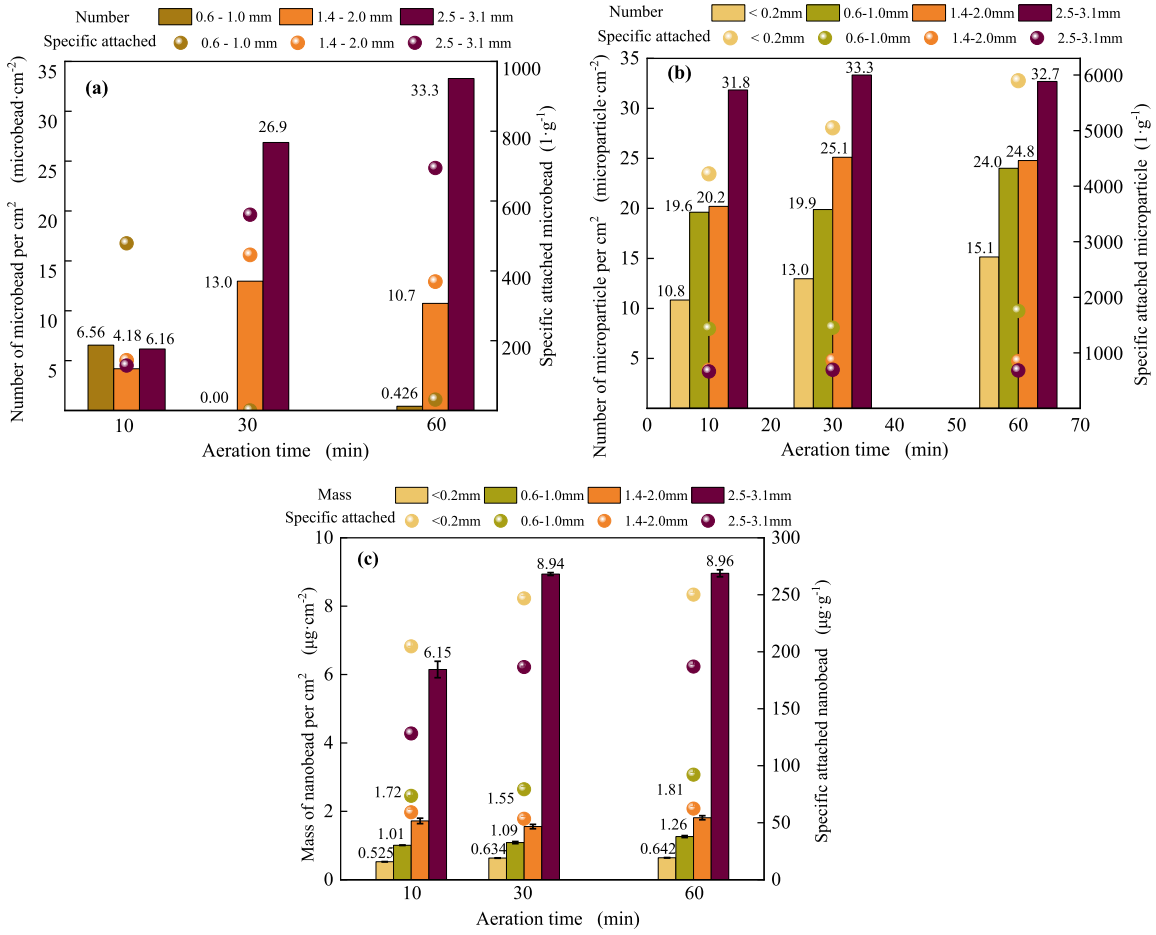

Fig. 4. The attached performance between different sized biomass and particles. (a) 250 μm microbeads; (b) 111±50 μm microparticles; (c) 100 nm nanobeads.

min of aeration with the attachment efficiency of 99±2 %, and almost did not change during the rest aeration. This indicated that nanobeads could be efficiently removed by the attachment onto the AGS mixture, although not all of them. The average specific attachment of 100 nm beads during aeration was around 34±0.4 $\mu g \cdot g^{-1}$.

3.3. The attachment between different sized particles and different sized biomass under mixed conditions

To investigate the interaction between different sized particles and different sized granules further, batch experiments were carried out to evaluate the attachment performance under mixed conditions. The density of AGS is in the range of 1025.7–1028.1 $kg \cdot m^{-3}$ (Van den Berg et al., 2023), in this study density of all granules was assumed as 1026.9 $kg \cdot m^{-3}$, and the equivalent diameters were 0.15 mm, 0.80 mm, 1.70 mm and 2.80 mm for sieve fractions of < 0.2 mm, 0.6–1.0 mm, 1.4–2.0 mm and 2.5–3.1 mm, respectively, the number of attached particles per cm^2 could be calculated (Fig. 4). The 250 μm microbeads attachment was not surface area related, and larger granules exhibited better attachment with the average specific attachment of 170, 319 and 461 microbeads$\cdot g^{-1}$ for sieve fractions of 0.6–1.0 mm, 1.4–2.0 mm and 2.5–3.1 mm, respectively. In addition, the number of attached microbeads per cm^2 by larger granules increased continuously during aeration, while it fluctuated for smaller granules. This was because the collisions between larger granules was stronger (Tijhuis et al., 1994), and some fragile parts would be peeled off from large granules to form new surface area. In this experiment, although we could not determine whether the microbead attached on large granules was detached from small granules or not, some large granules with a huge gap on the surface were indeed observed (Fig. 5(a)), as well as the peeled off layer (Fig. 5(b)).

The smaller granules had better attachment performance of 111±50 μm microparticles than larger granules. The average specific attached microparticles decreased with the increase of granule size (Fig. 4(b)), but there was little quantitative relation between the specific attachment and granule size (−0.900, p value 0.287). In addition, the microparticles attachment was very stable, and the number of the attached microparticles per cm^2 of all sized granules increased continuously during aeration. We observed that some microparticles deeply inserted into the soft granule surface (Fig. 5(c)). Furthermore, smaller granules attached more microparticles than the larger granules, with an average fraction of remaining suspended microparticles during 60 min aeration of 14±4 %, 19±6 %, 24±17 % and 65±29 % for sieve fractions < 0.2 mm (flocs), 0.6–1.0 mm, 1.4–2.0 mm and 2.5–3.1 mm, respectively (Table 2). And smaller microparticles were more prone to be attached than the larger ones. The average attached microparticles size were 138 ±43 μm, 113±48 μm, 111±43 μm and 135±24 μm, which were 13 %, 19 %, 26 % and 6 % smaller than those of remaining suspended microparticles, respectively. Meanwhile, the average △y/△x (the ratio of length to width) of suspended microparticles during 60 min aeration were 1.25±0.26, 1.22±0.25, 1.30±0.15 and 1.25±0.19, which were 0.5–7.4 % smaller than those of attached microparticles, indicating the irregularly shaped microparticles with smaller size were more likely to be attached.

Table 2
The characteristics of suspended and entrapped microparticles during aeration.

Aeration 60 min	Sieve fractions	Ratio (%)	Size (μm)	△y/△x
Suspended microparticles	< 0.2 mm	14 ± 4	158 ± 45	1.25 ± 0.26
	0.6 - 1.0 mm	19 ± 6	141 ± 44	1.22 ± 0.25
	1.4 - 2.0 mm	24 ± 17	149 ± 46	1.30 ± 0.15
	2.5 - 3.1 mm	65 ± 29	144 ± 55	1.25 ± 0.19
Entrapped microparticles	< 0.2 mm	86 ± 4	138 ± 43	1.35 ± 0.31
	0.6 - 1.0 mm	81 ± 6	113 ± 48	1.23 ± 0.24
	1.4 - 2.0 mm	76 ± 17	111 ± 43	1.30 ± 0.25
	2.5 - 3.1 mm	35 ± 29	135 ± 24	1.27 ± 0.11

The attachment between 100 nm nanobeads and different sized

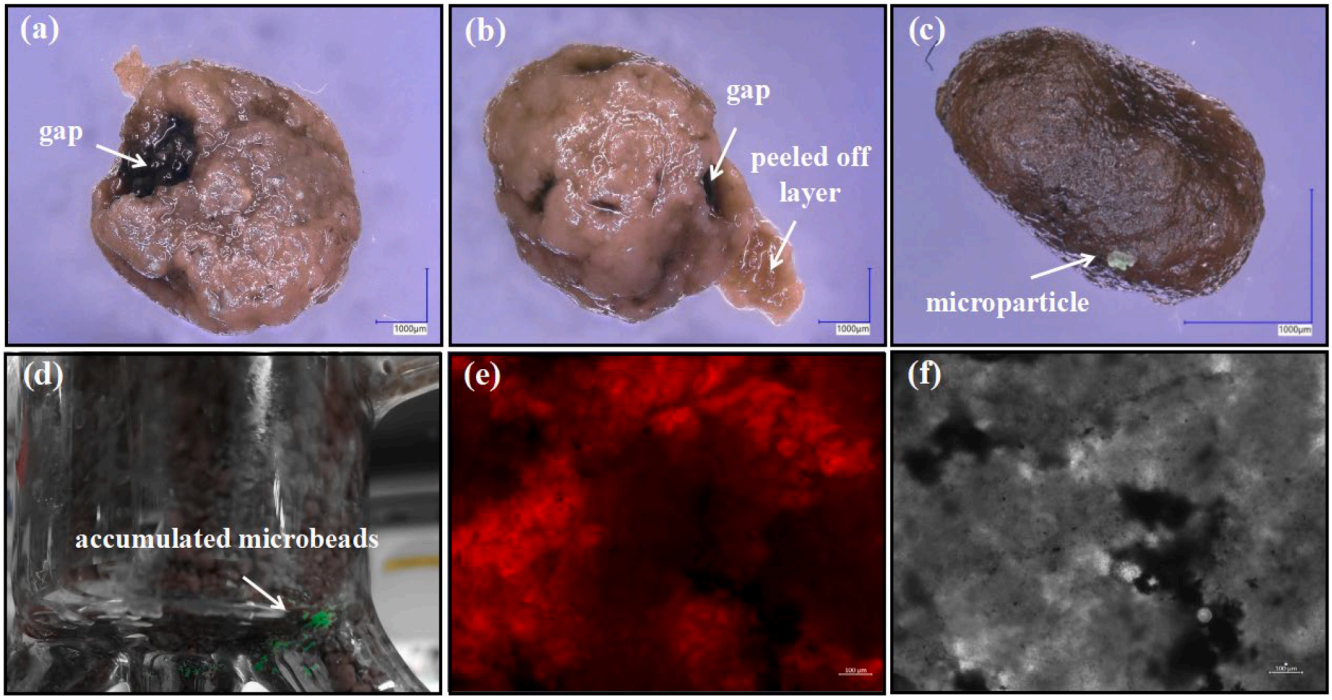

Fig. 5. Morphology of AGS surface (a) a gap on surface; (b) peeled off layers; (c) attached microparticle; (d) accumulated microbeads; (e) cy3 of AGS surface; (f) contrast of AGS surface.

granules also increased generally during aeration. Similar to the 111±50 μm microparticles, the nanobeads attachment also had no significant relation to the surface area of the granules (0.761, p value 0.239). For the sieve fractions <0.2 mm (flocs), 0.6–1.0 mm, 1.4–2.0 mm, and 2.5–3.1 mm, the average mass of attached nanobeads per cm^2 was 0.6, 1.1, 1.7 and 8.0 $\mu g \cdot cm^{-2}$ respectively, and the average specific attachment was respectively 234, 82, 58 and 167 $\mu g \cdot g^{-1}$. These data show that in this study the sludge flocs exhibited a better attachment performance than the small granules, while larger granules also exhibited excellent nanobeads attachment.

4. Discussion

4.1. Could the settled sludge bed perform as a filter during plug up-flow feeding?

Larger granules are more likely to settle faster to form a settled bed with smaller granules on the top and larger granules near the bottom during the settle phase. The filter performance is determined by the grain size, shape, and bed depth (L) to effective grain size (de) ratio. The range of L/de is usually bigger than 1000 (McGivney et al., 2008). In our study, the L/de was around 2000 with the L and de of 0.21 m and 109.1 μm, so the settled bed could be treated as a filter. The filtration mechanisms consisted of straining, sedimentation, interception, diffusion, etc., and the occurrence of each mechanisms is determined by the particle size (Yao et al., 1971). Since the 250 μm microbead was larger or close to the void of settled AGS bed, most was accumulated around the bottom (Fig. 5(d)). While most 130±58 μm microparticles can flow around the granules inside the sludge bed, and attached by the granules surface through sedimentation or interception. Specifically, the smaller microparticles in the distribution usually determine the filtration performance (Wakeman. 2007). Many pathogens in wastewater had similar size to the nanobeads in this study, such as E.coli, and they can quickly attach on the granule surface when passing through the settled sludge bed during anaerobic feeding (Barrios-Hernández et al., 2021). However, the particles smaller than 1 μm were dominantly transport by diffusion (Zamani and Maini., 2009), so some nanobeads flowing in the void can pass through the settled sludge bed. In this study the porosity of the settled sludge bed was around 50–60 %, and the filtration efficiency of nanobeads was 39–52 %, verifying the above research well. During the aeration period, the nanobeads could be removed with the average attachment efficiencies of 99±0.3 % through adsorption. This was also similar to the removal performance of MS2 bacteriophage, which size was only 27 nm (Thwaites et al., 2018). In addition, the effect of vital role of microorganisms can not be neglected in the filtration process (Corbera-Rubio et al., 2024). The protozoa predation mostly occurred during aerobic phase (Raboni et al., 2016), and in our study its contribution was limited since the washed AGS was saved in refrigerator under 5 °C before experiment .

4.2. Will the attached particles transfer from large granules to small granules during aeration?

Based on the specific attachment of particles to different sieve

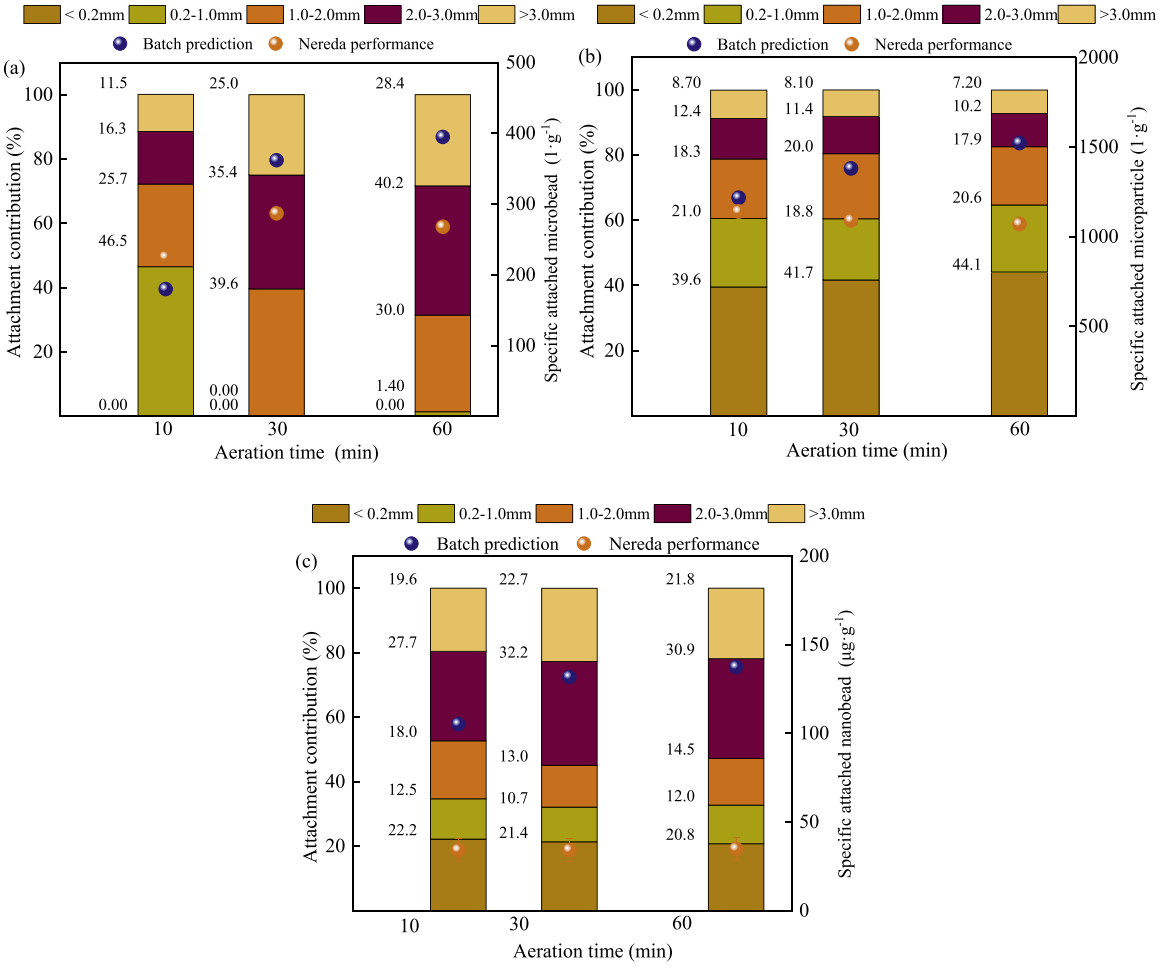

Fig. 6. The comparison of particles attachment by AGS mixture between prediction attachment and actual attachment (a) 250 μm microbeads; (b) 111±50 (130±58) μm microparticles; (c) 100 nm nanobeads.

fractions determined during the batch experiments, and the MLSS distribution of different sized AGS in the plug-flow feeding experiments, the particles attachment performance within AGS mixture during aeration was calculated. The comparasion of these calculations and the results of aeration after plug-flow feeding were shown in Fig. 6. The calculated specific attachment of the three fed particles increased during the aeration (blue dots). Interestingly, we calculated a shifted attachment behavior between the granule sizes that was most apparent for the smooth large spherical particles; it seemed that the microbeads attached to the smaller granules during the early period of aeration, then detached and re-attached to the larger granules (Fig. 6(a)). When the particles were medium with irregular shape, we calculated the microparticles captured by flocs increased from 40 % at 10 min to 44 % at 60 min aeration, and the microparticles attached to the largest fraction of granules decreased from 21 % after 10 min aeration to 17 % after 60 min. When the particles were small with regular shape, we calculated the attached nanobeads by flocs decreased from 22 % after 10 min aeration to 21 % after 60 min aeration, and the nanobeads attached to the largest fraction of granules increased from 47 % after 10 min aeration to 53 % after 60 min aeration. The reason for the slight variation is just that in general it is all balanced out (all the time a similar number of nanobeads attached).

The actual attachment performance during aeration after plug-flow feeding differed from the calculations. For the 250 μm microbeads, the specific attachment fluctuated in the range of 260±32 microbeads·g^{-1}, and the detachment and attachment played a major role in the removal of these microbeads, especially to the larger granules (Zhou et al., 2014). The binding between the microbeads and the granules is therefore considered low. For the 130±58 μm microparticles, the specific attachment already reached its maximum after 10 min aeration, and the contribution of the larger granules only decreased slightly during the rest phase. It is possible that the attachment of the irregular microparticles was strong, sometimes the embedding of microparticles were more into the AGS than on the AGS (Fig. 5(c)). While if the microparticles remained suspended, or detached from granules, they will be easily sweep removed by the flocculant sludge with more open structure (Ghernaout and Ghernaout, 2012). In our study, although the attachment between microparticles and AGS were strong, its contribution by flocs were still close to 50 %. Actually, in full-scale Nereda® plant a large contribution of flocculent sludge was found in the removal and hydrolysis of suspended solids (Toja Ortega et al., 2021), and the low stabilization of the flocculent sludge fraction upon anaerobic digestion could be also due to the captured organic microparticles in combination with short residence times (Guo et al., 2020).

The specific attached 100 nm nanobeads between the batch prediction and Nereda performance were not at the same level (Fig. 6(c)), the reason was the MLSS of the batch experiment were smaller. However, the variation trend of calculation aligned with that of plug flow feeding experiment. The specific nanobeads attachment of both increased during the first 30 min, and the contribution of larger granules in the nanobeads removal increased. The reason was the nanobeads were distributed very evenly and stably in the mixture, and the AGS required sufficient time to mix thoroughly after aeration, typically around 30 min (Toja Ortega et al., 2021). Furthermore, cracks and fissures would be produced on the surface of biofilm during aeration (Gjaltema et al., 1995), and the fissures on the surface of AGS can be as large as the nanobeads used in our study (Van den Berg., 2022). The mass transfer inside the granules was heterogeneous (Van den Berg et al., 2020), and the nanobeads diffusion inside the AGS would not be hampered obviously (Ahn et al., 2015), so nanobeads were attached by both outer surface and internal surface (Wang et al., 2021). Especially in the voids of granules where the nanobeads encounter lower shear and lower detachment chances (Picioreanu et al., 2004; Ranzinger et al., 2020). While the internal surface attachment would not happen for bigger substrates such as suspended starch (De Kreuk et al., 2010). Furthermore, the AGS surface was not smooth caused by the alginate-like exopolysaccharides induced struvites (Lin et al., 2012), and the roughness distribution on the AGS outer surface was uneven (Fig. 5(e),(f)), which was verified by the bright red area (amyloid-glucan structure). According to this attachment ability in this study, if the MLSS was 6000–10,000 mg·L^{-1} in Nereda® system, the maximum influent nanobeads that can be effectively removed was 180–300 μg·L^{-1}.

4.3. The evaluation of waste AGS sludge treatment

The particles used in this study were actually micro/nano plastics, which removal in wastewater treatment are gaining attention. In this study, 45±5 % of the microbeads, 92±3 % of the microparticles, and 99 ±0.3 % of the nanobeads were attached to the AGS after 60 min aeration. What is the fate of these attached particles in the waste sludge processing? During the activated sludge dewatering process, 95 % of attached microplastic were retained due to size-limited transport, while around 50 % of nanoplastic were released through the co-transport with the mobile organic fraction (Keller et al., 2020). Considering the microbeads attachment was weak, we could assume the attached microbeads by AGS will easily detach by the shear forces. For the activated sludge, the concentration of microplastics based leachates in sludge is 2–25 times bigger than that in water (Yang et al., 2024). Although the dewatering performance of AGS is better (Yan et al., 2024), the behavior of microparticles and nanobeads during AGS dewatering was still not clear so far.

Anaerobic digestion is a well-applied technology to diminish the amount of excess sludge and recover energy (Sun et al., 2019). Micro/nano zero-valent iron could be added to enhance the anaerobic digestion processes, such as hydrolysis, acidification and methanogenesis (Lu et al., 2016). Although it was difficult to observe the specific attached micro/nano iron on the sludge, the production of volatile fatty acids and methane were improved obviously during long-term operation (Feng et al., 2014), this indirectly verified the micro/nano particles can be attached to biomass firmly in anaerobic digestion. Incineration can reduce the amount of sludge maximally by converting the inorganic matter to ash (Liang et al., 2021). Compared with other treatment methods, incineration is relatively expensive due to investment and operational costs (energy consumption of drying and control of NO_x and SO_2 emissions). On the other hand, sanitary landfill has become less used due to limited space availability (Hao et al., 2020).

When disposing the waste activated sludge treated by anaerobic digestion or dewatering only, strategy should be done to prevent the secondary pollution of micro/nano particles. However, whether the behaviour of micro/nano particles in AGS were the same as in the activated sludge waste treatment was still not clear. On the other hand, when the micro/nano particles of the dewatered sludge are oxidized during incineration, whether the extra oxidation to CO_2 or H_2O bring any consequence, or is it comparable to the sludge oxidation in volume? These are all need to be verified further.

4.4. The evaluation of the fate of influent pCOD in Nereda® systems

Even though this study used fluorescent microbeads and nanobeads to stimulate influent non-biodegradable pCOD, the obtained results could also provide insight to the removal of biodegradable and non-biodegradable pCOD during wastewater treatment. Particles in domestic sewage are characterized by an irregular morphology (Keller et al., 2020), and most pCOD size fall within the 10–150 μm (Hocaoglu et al., 2013), which are simialr to the 130±58 μm microparticles in this study. Meanwhile, the AGS collected from a full-scale Nereda® plant with stable operation, and there are some other research also use the Utrecht AGS to do batch experiments (Feng et al., 2024). So when a Nereda® system was used to treat actual domestic wastewter, the fate of influent pCOD was expected to be similar to the microparticles in this study. According to the results of Sections 3.2 and 3.3, most microparticles were strongly attached by the biomass during aeration, especially the

smaller granules or flocculent sludge. Therefore, most influent non-biodegradable pCOD will be removed by discharging the waste AGS. In line with the findings of Toja-Ortega et al. (2022), we can assume that the biodegradable pCOD, on the other hand, can attach to the granules and be slowly degraded by the granules due to their usually long solid retention times. In the full scale Nereda® plant of Garmerwolde, the solid retention time was 20–38 d (Pronk et al., 2015), which was much bigger than that of conventional activated sludge system.

Furthermore, there are many research focusing on improving granulation in continuous flow systems (Yu et al., 2024; Haaksman et al., 2023). Since most organics of actual sewage existed as pCOD with similar size to the microparticles and nanobeads in our study (Hocaoglu et al., 2013), and both of them could be firmly attached by AGS under mixing condition, it is essential to guarantee these particles preferentially be attached by larger AGS. However, the smaller granules and flocs with bigger specific surface area are more prone to attach the influent pCOD. So, it would be possible to create a "periodic larger biomass preferentially contact influent" in the anaerobic tank through the intermittent anaerobic mixing (on-off) and bottom feeding, while the balance between granulation and treatment performance should be evaluated further in-depth.

5. Conclusions

This study investigated the interactions between 250 μm microbeads, 130±58 μm microparticles, 100 nm nanobeads and granular sludge in Nereda®. During the plug-flow feeding phase, the filtration performance of settled AGS bed was mainly influenced by the particle size. Most 250 μm microbeads were accumulated around the bottom with a filtration efficiency of 91–98 %, while only 41–52 % of 100 nm nanobeads were filtered out. During the aeration phase, the large and smooth microbeads revealed a relatively low attachment efficiency (39–49 %), while both the microparticles (89.4–95.2 %) and nanobeads (98.8–99.3 %) could be firmly attached by the biomass, and the transfer of the attached microparticles/nanobeads between different sized AGS was very limited. Specifically, the smaller and irregular microparticles more likely attached to small AGS and sludge flocs, and the nanobeads preferentially attached to sludge flocs and large AGS. The interaction between different-sized particles and AGS in Nereda® during long-term operation need to be investigated in the future.

CRediT authorship contribution statement

Zhaoxu Peng: Writing – review & editing, Writing – original draft, Validation, Methodology, Investigation, Funding acquisition, Data curation, Conceptualization. **Antonella L. Piaggio:** Validation, Methodology. **Guilherme Lelis Giglio:** Validation, Methodology, Data curation. **Sara Toja Ortega:** Validation. **Mark C.M. van Loosdrecht:** Validation, Formal analysis, Data curation, Conceptualization. **Merle K. de Kreuk:** Validation, Supervision, Methodology, Conceptualization.

Declaration of competing interest

The authors declare that they have no known competing financial interests or personal relationships that could have appeared to influence the work reported in this paper.

Acknowledgments

This research was supported by the China Scholarship Council (No. 202107045010). We thank the colleagues of water lab, TU Delft, for their great help, especially to Armand Middeldorp for his contribution in the optimal use of Laboratorium equipment. We also thank Mark Stevens for his help during sampling and discussion in the Utrecht sewage treatment plant.

Data availability

Data will be made available on request.

References

Ahn, K.H., Hong, S.W., 2015. Characteristics of the adsorbed heavy metals onto aerobic granules: isotherms and distributions. Desalin. Water Treat. 53, 2388–2402.
Alvarado, A., West, S., Abbt-Braun, G., Horn, H., 2021. Hydrolysis of particulate organic matter from municipal wastewater under aerobic treatment. Chemosphere. 263, 128329.
APHA, 2005. Standard Methods for the Examination of Water and Wastewater, 21sted. American Public Health Association, Washington, DC.
Barrios-Hernández, M.L., Bettinelli, C., Mora-Cabrera, K., Vanegas-Camero, M.C., Hooijmans, C.M., 2021. Unravelling the removal mechanisms of bacterial and viral surrogates in aerobic granular sludge systems. Water Res. 195, 116992.
Beun, J.J., van Loosdrecht, M.C.M., Heijnen, J.J., 2002. Aerobic granulation in a sequencing batch airlift reactor. Water Res. 36, 702.
Corbera-Rubio, F., Goedhart, R., Laureni, M., van Loosdrecht, M.C.M., van Halem, D., 2024. A biotechnological perspective on sand filtration for drinking water production. Curr. Opin. Biotechnol. 90, 103221.
De Kreuk, M.K., Kishida, N., Tsuneda, S., van Loosdrecht, M.C.M., 2010. Behavior of polymeric substrates in an aerobic granular sludge system. Water Res. 44 (20), 5929–5938.
De Kreuk, M.K., Kishida, N., Van Loosdrecht, M.C.M., 2007. Aerobic granular sludge–state of the art. Water Sci Technol 55 (8–9), 75–81.
Elahinik, A., Haarsma, M., Abbas, B., Pabst, M., Xevgenos, D., Van Loosdrecht, M.C.M., Pronk, M., 2022. Glycerol conversion by aerobic granular sludge. Water Res. 227, 119340.
Feng, Y.H., Zhang, Y.B., Quan, X., Chen, S., 2014. Enhanced anaerobic digestion of waste activated sludge digestion by the addition of zero valent iron. Water Res. 52, 242–250.
Feng, Z.L., Schmitt, H., Van Loosdrecht, Sutton, N.B., 2024. Sludge size affects sorption of organic micropollutants in full-scale aerobic granular sludge systems. Water Res. 267, 122513.
Ghernaout, D., Ghernaout, B., 2012. Sweep flocculation as a second form of charge neutralisation-a review. Desalin. Water Treat. 44, 15–28.
Gjaltema, A., Tijhuis, L., van Loosdrecht, M.C.M., Heijnen, J.J., 1995. Detachment of biomass from suspended nongrowing spherical biofilms in airlift reactors. Biotechnol. Bioeng. 46, 258-269.
Guo, H.X., van Lier, J.B., de Kreuk, M.K., 2020. Digestibility of waste aerobic granular sludge from a full-scale municipal wastewater treatment system. Water Res. 173, 115617.
Haaksman, V.A., Schouteren, M., Van Loosdrecht, M.C.M., Pronk, M., 2023. Impact of the anaerobic feeding mode on substrate distribution in aerobic granular sludge. Water Res. 233, 119803.Y.
Hao, X.D., Chen, Q., van Loosdrecht, M.C.M., Li, J., Jiang, H., 2020. Sustainable disposal of excess sludge: incineration without anaerobic digestion. Water Res. 170, 115298.
Hocaoglu, S.M., Orhon, D., 2013. Particle size distribution analysis of chemical oxygen demand fractions with different biodegradation characteristics in black water and gray water. Clean-Soil Air Water. 41 (11),1044-1051.
Jia, T.L., Peng, Z.X., Yu, J., Piaggio, A.L., Zhang, S., De Kreuk, M.K., 2024. Detection the interaction between microparticles and biomass in biological wastewater treatment process with deep learning method. Sci. Total Environ. 951, 175813.
Karahan, O., Dogruel, S., Dulekgurgen, E., Orhon, D., 2008. COD fractionation of tannery wastewaters—particle size distribution, biodegradability and modeling. Water Res. 42, 1083–1092.
Keller, A.S., Jimenez-Martinez, J., Mitrano, D.M., 2020. Transport of nano- and microplastic through unsaturated porous media from sewage sludge application. Environ. Sci. Technol. 54 (2), 911–920.
Layer, M., Bock, K., Ranzinger, F., Horn, H., Morgenroth, E., Derlon, N., 2020. Particulate substrate retention in plug-flow and fully-mixed conditions during operation of aerobic granular sludge systems. Water Res. X 9, 100075.
Liang, Y., Xu, D.H., Feng, P., Hao, B.T., Guo, Y., Wang, S.Z., 2021. Municipal sewage sludge incineration and its air pollution control. J. Clean Prod. 295, 126456.
Lin, Y.M., Bassin, J.P., van Loosdrecht, M.C.M., 2012. The contribution of exopolysaccharides induced struvites accumulation to ammonium adsorption in aerobic granular sludge. Water Res. 46 (4), 986–992.
Lu, H.J., Wang, J.K., Ferguson, S., Wang, T., Bao, Y., Hao, H.X., 2016. Mechanism, synthesis and modification of nano zerovalent iron in water treatment. Nanoscale 8 (19), 9962–9975.
McGivney, W., Kawamura, S., 2008. Cost Estimating Manual For Water Treatment Facilities. John Wiley & Sons, Inc., Hoboken, NJ, USA.
Picioreanu, C., Kreft, J.U., van Loosdrecht, M.C.M., 2004. Particle-based multidimensional multispecies biofilm model. Appl. Environ. Microbiol. 70 (5), 3024–3040.
Pronk, M., De Kreuk, M., De Bruin, B., Kamminga, P., Kleerebezem, R., Van Loosdrecht, M.C.M., 2015. Full scale performance of the aerobic granular sludge process for sewage treatment. Water Res. 84, 207–217.
Raboni, M., Gavasci, R., Torretta, V., 2016. Assessment of the fate of *Escherichia coli* in different stages of wastewater treatment plants. Water Air Soil Pollut. 227, 455.
Ranzinger, F., Matern, M., Layer, M., Guthausen, G., Wagner, M., Derlon, N., Horn, H., 2020. Transport and retention of artificial and real wastewater particles inside a bed

of settled aerobic granular sludge assessed applying magnetic resonance imaging. Water Res. X 7, 100050.
Sun, J., Dai, X., Wang, Q., van Loosdrecht, M.C.M., Ni, B.-J., 2019. Microplastics in wastewater treatment plants: detection, occurrence and removal. Water Res. 152, 21–37.
Thwaites, B.J., Short, M.D., Stuetz, R.M., Reeve, P.J., Gaitan, J-P.A., Dinesh, N., van den Akker, B., 2018. Comparing the performance of aerobic granular sludge versus conventional activated sludge for microbial log removal and effluent quality: implications for water reuse. Water Res. 145, 442–452.
Tijhuis, L., van Loosdrecht, M.C.M., Heijnen, J.J., 1994. Formation and growth of heterotrophic aerobic biofilms on small suspended particles in airlift reactors. Biotechnol. Bioeng. 44, 595-608.
Toja Ortega, S., Pronk, M., de Kreuk, M.K., 2021. Effect of an increased particulate COD load on the aerobic granular sludge process: a full scale study. Processes 9 (8), 1472.
Toja Ortega, S., van den Berg, L., Pronk, M., de Kreuk, M.K., 2022. Hydrolysis capacity of different sized granules in a full-scale aerobic granular sludge (AGS) reactor. Water Res. X 16, 100151.
Van den Berg, L., Kirkland, C.M., Seymour, J.D., Codd, S.L., van Loosdrecht, M.C.M., de Kreuk, M.K., 2020. Heterogeneous diffusion in aerobic granular sludge. Biotechnol. Bioeng. 117, 3809–3819.
Van den Berg, L., Ortega, S.T., van Loosdrecht, M.C.M., de Kreuk, M.K., 2022. Diffusion of soluble organic substrates in aerobic granular sludge effect of molecular weight. Water Res. 16, 100148.
Van den Berg, L., Pronk, M., van Loosdrecht, M.C.M., de Kreuk, M.K., 2023. Density measurements of aerobic granular sludge. Environ. Technol. 44 (13), 1985–1995.
Van Dijk, E.J.H., Haaksman, V.A., Van Loosdrecht, M.C.M., Pronk, M., 2022. On the mechanisms for aerobic granulation - model based evaluation. Water Res. 216, 118365.
Wakeman, R., 2007. The influence of particle properties on filtration. Sep. Purif. Technol. 58, 234–241.
Wang, Q.H., Yan, G.X., Cai, B., Chen, C.M., Guo, S.H., 2014. Characterization of dry-spun acrylic fiber wastewater by particle size distribution, biodegradability, and chemical composition. Clean Soil Air Water 42 (10), 1393–1401.
Wang, X.C., Li, J., Zhang, X.L., Chen, Z.L., Shen, J.M., Kang, J., 2021. Effect of aerobic granular sludge concentrations on adsorption and biodegradation to oxytetracycline. Water Air Soil Pollut. 232, 184.
Winkler, K.H., Van Loosdrecht, M.C.M., 2022. Intensifying existing urban wastewater aerobic granular sludge offers improvements to treatment processes. Science 375 (6579), 377–378.
Yan, A.L., Chen, Y.F., Li, N.Y., Ma, T., Qi, Y.T., Xu, D., 2024. Dewatering performance of aerobic granular sludge under centrifugal with different sludge conditioning agent. Front. Microbiol. 15, 1386557.
Yang, X.F., Niu, S.Y., Li, M., Niu, Y.L., Shen, K.L., Dong, B., Hur, J., Li, X.W., 2024. Leaching behavior of microplastics during sludge mechanical dewatering and its effect on activated sludge. Water Res. 266, 122395.
Yao, K.M., Habibian, M.T., O'Melia, C.R., 1971. Water and waste water filtration. Concepts and applications. Environ. Sci. Technol. 5, 1105–1112.
Yu, C., Wang, K.J., Zhang, K.Y., Liu, R.Y., Zheng, P.P., 2024. Full-scale upgrade activated sludge to continuous-flow aerobic granular sludge: implementing microaerobic-aerobic configuration with internal separators. Water Res. 248, 120870.
Zamani, A., Maini, B., 2009. Flow of dispersed particles through porous media—deep bed filtration. J. Pet. Sci. Eng. 69, 71–88.
Zhou, D.D., Niu, S., Xiong, Y.J., Yang, Y., Dong, S.S., 2014. Microbial selection pressure is not a prerequisite for granulation: dynamic granulation and microbial community study in a complete mixing bioreactor. Bioresour. Technol. 161, 102–108.